

Heat-induced ribosome pausing triggers mRNA co-translational decay in *Arabidopsis thaliana*

Rémy Merret^{1,2}, Vinay K. Nagarajan^{3,†}, Marie-Christine Carpentier^{1,2,†}, Sunhee Park³, Jean-Jacques Favory^{1,2}, Julie Descombin^{1,2}, Claire Picart^{1,2}, Yee-yung Charng⁴, Pamela J. Green³, Jean-Marc Deragon^{1,2} and Cécile Bousquet-Antonelli^{1,2,*}

¹CNRS-LGDP UMR 5096, 58 av. Paul Alduy 66860 Perpignan, France, ²Université de Perpignan Via Domitia, LGDP-UMR5096, 58 av. Paul Alduy, 66860 Perpignan, France, ³University of Delaware, Delaware Biotechnology Institute, 15 Innovation Way, Newark, DE 19711, USA and ⁴Agricultural Biotechnology Research Center, Academia Sinica, 128 Academia Road Section 2, Taipei, Taiwan 11529, ROC

Received January 09, 2015; Revised February 18, 2015; Accepted March 06, 2015

ABSTRACT

The reprogramming of gene expression in heat stress is a key determinant to organism survival. Gene expression is downregulated through translation initiation inhibition and release of free mRNPs that are rapidly degraded or stored. In mammals, heat also triggers 5'-ribosome pausing preferentially on transcripts coding for HSC/HSP70 chaperone targets, but the impact of such phenomenon on mRNA fate remains unknown. Here, we provide evidence that, in *Arabidopsis thaliana*, heat provokes 5'-ribosome pausing leading to the XRN4-mediated 5'-directed decay of translating mRNAs. We also show that hindering HSC/HSP70 activity at 20°C recapitulates heat effects by inducing ribosome pausing and co-translational mRNA turnover. Strikingly, co-translational decay targets encode proteins with high HSC/HSP70 binding scores and hydrophobic N-termini, two characteristics that were previously observed for transcripts most prone to pausing in animals. This work suggests for the first time that stress-induced variation of translation elongation rate is an evolutionarily conserved process leading to the polysomal degradation of thousands of 'non-aberrant' mRNAs.

INTRODUCTION

At the cellular level, heat exposure triggers a global down-regulation of gene expression while promoting the selective synthesis of stress-related proteins (1). At the organism level, these changes allow for the setting up of new metabolic programs that enable acclimation and survival

(2,3). Translation, which consumes a lion's share of energy, is one of the first processes to be downregulated upon temperature increase. Translation inhibition is commensurate to stress intensity and duration and is the consequence of translation initiation impediment through molecular determinants that yet remain unclear in plants (4,5). In mammalian cells, heat and proteotoxic stresses also affect translation at the elongation step. Stress-induced alterations of the cellular environment, especially the increased accumulation of misfolded proteins, provoke a ribosome trapping mechanism or '5'-ribosome pausing' (6,7). This phenomenon, which temporarily arrests elongation around codon 65, is seemingly the direct consequence of the decreased availability at polysomes of HSC70/HSP70 chaperones (6,7), which act to assist the co-translational folding of emerging polypeptides at the ribosome exit tunnel (6–10).

In the cytoplasm, the general mRNA turnover process occurs through an evolutionarily conserved deadenylation-dependent mechanism. After poly(A) tail shortening, the body of the transcript is degraded exonucleolytically from its 3' and/or 5' end (11–14). The 5'-turnover process involves, following deadenylation, a decapping step through which the 5'-m⁷Gpp protecting structure is excised gaining access to the cytoplasmic 5'–3' exoribonuclease XRN1 (XRN4 in *Arabidopsis*) (15–18). So far, the main decapping activity was found to be carried by the DCP1/HEDLS(AtVCS)/DCP2 holoenzyme (19), and its functional homolog was identified in *Arabidopsis* (20,21). mRNA stability control and reprogramming play an important role in the adaptation of the cell to stressful conditions (22). We recently provided evidence that, in *Arabidopsis thaliana*, heat exposure induces a Heat-Stress Mediated Decay (H-SMD), which we proposed to be at least in part responsible for the downregulation through destabilization of several thousand mRNAs (representing 25% of the plant

*To whom correspondence should be addressed. Tel: +33 468662247; Fax: +33 468668499; Email: cecile.antonelli@univ-perp.fr

†These authors contributed equally to the paper.

Present address: Rémy Merret, Agricultural Biotechnology Research Center, Academia Sinica, 128 Academia Road Section 2, Taipei, Taiwan 11529, ROC.

transcriptome) mostly coding for housekeeping functions (23). We posit a model in which baits of the H-SMD are targeted to a rapid 5'–3' oriented degradation, catalyzed during heat stress by a functionally reprogrammed XRN4 enzyme (23).

Translation and mRNA degradation are intertwined and have long been thought to simply be inversely correlated; the model being that translating mRNAs were protected from degradation (24,25). Consistently, stress-induced translation initiation impediment releases free mRNPs which aggregate into p-body (processing body) granules that concentrate mRNA decapping and degradation factors and cofactors (26,27). While p-bodies are decapping and degradation centers of mRNPs (28) and their increase in size and number fits with an increased mRNA turnover activity in stress situation, things are not always as straightforward (24,25). Indeed, translation initiation inhibition and polysome disengagement are not systematically synonymous to mRNA decay in particular in response to stress situation where mRNPs can also be transiently stored as ribosome-free complexes in p-bodies or as pre-initiation complexes in stress granule (SG) (29–31). Moreover, full polysome dissociation is not always a prerequisite for mRNA degradation. Studies conducted in *Saccharomyces cerevisiae* revealed the existence of a co-translational decay mechanism in which non-aberrant transcripts can be decapped and subsequently 5'-digested by Xrn1p while ribosomes are finishing elongation (32). Consistently with the putative existence of such process in other eukaryotes, actors of the 5'-decay apparatus were found to associate with translating ribosomes in mammals (33) and higher plants (23). Nevertheless although it seems to be evolutionarily conserved neither the cellular importance nor target specificity of this process is clearly defined at present.

In the present study, we investigate the involvement of XRN4 in the putative heat triggered polysomal degradation of mRNAs in *A. thaliana*. We conducted RNA-seq analyses to qualitatively and quantitatively assess the requirement of XRN4 for the heat-induced downregulation of mRNAs in polysomes. Our analyses show that more than 85% of transcripts downregulated at 38°C in polysomes accumulate to higher levels in an *xrn4* mutant background. Using randomly chosen mRNAs, we demonstrate that heat and XRN4 depletion induce the overaccumulation of decapped intermediates in polysomes. We present data supporting that, as it is the case in mammals, heat provokes a 5'-ribosome pausing phenomenon and show that a drug-mediated inhibition of HSC70/HSP70 chaperone activities also induces pausing and XRN4 catalyzed polysomal degradation at 20°C. Overall, we provide strong evidence that, for a subclass of mRNAs preferentially coding for proteins with highly hydrophobic N-termini targeted by HSC70/HSP70, heat triggers 5'-ribosome pausing which in turn induces XRN4-mediated polysomal decay.

MATERIALS AND METHODS

Arabidopsis growth and treatments

We used either wild-type Columbia 0 or *xrn4-5* (SAIL_681E01) full knock-out mutant (18). Analyses were carried out with 21 day old whole seedlings grown on

synthetic Murashige and Skoog (MS) medium (MS0213 from Duchefa) containing 1% sucrose and 0.8% plant agar at 20°C under continuous light. Heat stress was carried as follow: six to eight plantlets were transferred to 5 ml liquid MS medium-1% sucrose. Light-grown plants were incubated for 30 min at 38°C while control plants were kept at 20°C for 30 min. For HSP70 inhibition, VER-155008 (Sigma SML0271) resuspended in DMSO was used at a final concentration of 100 µM. Plants were incubated as described above in the presence of inhibitor or with 0.1% DMSO (control treatment) for 60 min at 20°C.

Polysome profile analysis, input and polysomal RNA purification

Polysome extraction was performed as described previously (23,34) with few modifications. Heparin was systematically omitted from the polysomal extraction buffer. Polysomal extracts (1.2 g equivalent biomass) were resolved on a 15–60% sucrose gradient (27 ml) centrifuged for 3.5 h at 30 000 rpm with rotor SW32 Ti. Polysome profile analyses were performed with an ISCO absorbance detector at 254 nm and sucrose gradient collected into 16 fractions of 2 ml each: fractions 1–4 containing free mRNPs, fractions 5–8 free ribosomes and 80S and fractions 9–16 polyribosomes. Values of absorbance at 254 nm were recorded with the Peak Track software, and polysome profiles represented as graphs with the Excel software. To determine the content in light polysome fractions relative to the total polysome content, the area covered beneath the peak(s) of interest was measured with Image J.

To extract RNA from sucrose gradient fractions (polysomal RNA) or crude polysomal extract (Input RNA), samples were homogenized with two volumes of 8M guanidium-HCl buffer (35) and three volumes of absolute ethanol and precipitated overnight at –20°C. After centrifugation (45 min at 16 000 rpm), pellets were homogenized in RLT buffer (RNeasy Mini Kit, Qiagen) and purification conducted according to manufacturer's instructions. Polyribosomal RNAs were extracted from pooled fractions 10 to 15 of the gradient, light and heavy polysomal RNAs from pooled fractions 10–12 and 13–15, respectively.

RNA-seq, qRT-PCR and SL-RT-PCR analyses

RNA-seq analyses were conducted in duplicate either on RNA extracted from total crude extract (Input) or from total polyribosomes (Polysomal) and are detailed in Supplementary Figure S1 and supplemental methods. For qRT-PCR, reverse transcription was conducted on 0.5 µg of DNase treated RNAs (Turbo DNase Ambion) using the Superscript III (Invitrogen) and an oligo(dT)₁₈ for priming. Real-time PCRs were performed in a LC 480 384-well device as in (23). qPCR results were obtained from three independent biological samples always conducted in technical replicates. Splinted Ligation Reverse Transcription PCRs (SL-RT-PCRs) were performed as described previously (36). For a detailed protocol and design of the splint DNA primers, see the supplemental methods. For both qRT-PCR and SL-RT-PCR primer sequences, see Supplementary Table S2.

Hydrophobicity and HSC/HSP70 scores

Hydrophobicity and HSC/HSP70 scoring were performed as in (7). Protein sequences encoded by class I and class III mRNAs that are specific targets of XRN4 in input and polysomes respectively were downloaded from TAIR10 and scores were calculated. Briefly, Kyte-doolittle hydrophobicity scores and HSC/HSP70 binding scores were respectively calculated on 13 amino acid long windows that were slid by 1 amino acid from N- to C-terminus of the first 80 amino acids of every proteins encoded by class I and class III genes. Mean values were calculated respectively in each class out of the values obtained for each gene and curves were fitted with the cubic spline interpolation mathematical function. A t-test was performed between each pair of population.

RESULTS

We prepared polysomal extracts from wild-type and *xrn4-5 null* seedlings incubated for 30 min, either at 20°C for non-stressed or 38°C for heat stress conditions. RNA-seq analyses were subsequently performed on poly(A) purified RNA extracted either from the total crude extracts (Input) or from fractions containing the polyribosomes collected after sucrose gradient separation (Polysomal) (see Supplementary Figure S1 and supplemental methods). After filtering, we retrieved more than 19 200 mRNAs with above threshold signal in the input and polysomal libraries, covering more than 70% of the predicted number of Arabidopsis genes (Supplementary Table S1). Each set of experiment was found to be reproducible as demonstrated by plotting read counts pairwise between replicates (with $0.84 < R^2 < 1$) (Supplementary Figure S2A–H). To assess the impact of the heat treatment on mRNA levels, we calculated a fold (F) obtained by dividing the number of reads at 38°C (q^{38°) by the number of reads at 20°C (q^{20°) and retained mRNAs with $F > 2$ for up- and $F < 0.5$ for downregulation criteria. Since we observed a good reproducibility of the folds between replicates (Supplementary Figure S2I–L), we used the average of the fold values between replicates ($_{av}F$) for all our analyses. As expected, heat induces the overaccumulation of 4% of the detected transcripts, which mostly code for heat and abiotic stress response factors. XRN4 does not seem to have a major regulatory impact on this effect, as shown by analyses of the upregulation response in the *xrn4-5* background (Supplementary Table S1 and data not shown). We therefore focused our attention on the impact of XRN4 in the heat triggered downregulation process.

Heat induces a massive XRN4-dependent downregulation response in input and polysomes

In polysomes from wild-type seedlings, heat stress triggers the downregulation of some 4000 mRNAs (precisely 4012 mRNAs Supplementary Table S1, Figure 1A). Their fold ($_{av}F$) change ranging between 0.5 and 0.007 (mean of 0.33), with 90% of them displaying an $_{av}F$ between 0.5 and 0.2. In polysomes from *xrn4-5* seedlings, 56.8% of them remain significantly decreased (i.e. with $_{av}F^{xrn4-5} < 0.5$) while 41.6% have an $_{av}F^{xrn4-5}$ between 0.5 and 1 and 1.6% an $_{av}F^{xrn4-5} > 1$ (Supplementary Table S1, Figure 1B). A direct comparison of their fold change in *xrn4-5* and wild-type polysomes

through calculation of the $\log_2(_{av}F^{WT}/_{av}F^{xrn4-5})$ shows that almost 85% have a negative \log_2 value (Figure 1B and D). At 20°C, XRN4 has globally no impact on the accumulation of these mRNAs in polysomes (Supplementary Figure S3A) but at 38°C, their levels are globally higher in *xrn4-5* than in wild-type (Supplementary Table S1 and Figure S3B). All these results suggest that the heat-induced under-accumulation of transcripts in polysomes is, at least in part, dependent upon XRN4 function.

In the input fraction from wild-type seedlings, almost 4500 mRNAs (precisely 4343 mRNAs) are downregulated by heat (Figure 1A, Supplementary Table S1). Their fold ($_{av}F$) change ranging between 0.5 and 0.017 (mean of 0.33), with 94% of them displaying an $_{av}F$ between 0.5 and 0.2. The extent and magnitude of this effect are both consistent with our previous study (23) and 58% of the present dataset significantly overlaps (P -value $5.8.10^{E-4}$, calculated testing the hypergeometric distribution) with the former one (Supplementary Figure S3C), despite the fact that stress conditions were partly distinct. Indeed in our former analysis plantlets were heat stressed in the dark (23), while in the present study we focused more precisely on the impact of heat alone. Heat stress was performed by treating seedlings at 38°C but with the same light conditions as the control conditions. As for the polysomal mRNAs, we evaluated the impact of XRN4 knockout on the input fraction and observed that 46.5% of the heat targets remain significantly decreased while 49.5% display fold change between 0.5 and 1 and 4% an $_{av}F^{xrn4-5} > 1$ (Supplementary Table S1). In addition, most of them (86%) have a negative $\log_2(_{av}F^{WT}/_{av}F^{xrn4-5})$ value (Figure 1C and D). At 20°C, XRN4 has globally no impact on their quantities (Supplementary Figure S3D) but at 38°C, their levels are globally higher in *xrn4-5* than in wild-type (Supplementary Table S1 and Figure S3E). Hence, in input also, the heat-induced downregulation appears to be, at least in part, dependent upon XRN4 function.

We next compared the lists of mRNAs sensitive to XRN4 in input and in polysomes, and found three classes of transcripts. Class I and class III encompass transcripts which $_{av}F$ is higher in *xrn4-5* seedlings than in wild-type in input and polysomes, respectively, while class II encompass transcripts which $_{av}F$ is increased by XRN4 knockout in both fractions (Figure 1D, Supplementary Table S1). Although the input fraction is a total extract encompassing cytoplasmic, polysomal and nuclear transcripts, class I mRNAs must be affected by XRN4 depletion mainly outside polysomes (otherwise an effect would show on polysomal libraries) and for direct targets of the exoribonuclease probably in the cytoplasm, since XRN4 is mainly a cytoplasmic enzyme (16,17,27). Class III transcripts are only significantly affected by XRN4 inactivation in polysomes, while class II mRNAs are affected either exclusively in polysomes but with a strong enough magnitude to also be detected in the total fraction, or both in polysomes and cytoplasm.

To further strengthen these observations, we monitored the fold change ($q^{38^\circ C}/q^{20^\circ C}$) in mRNA levels by quantitative RT-PCR (qRT-PCR) (Figure 1E, Supplementary Figure S3F). Input and polysomal RNAs were purified as for the transcriptomic analyses but from a new set of biological

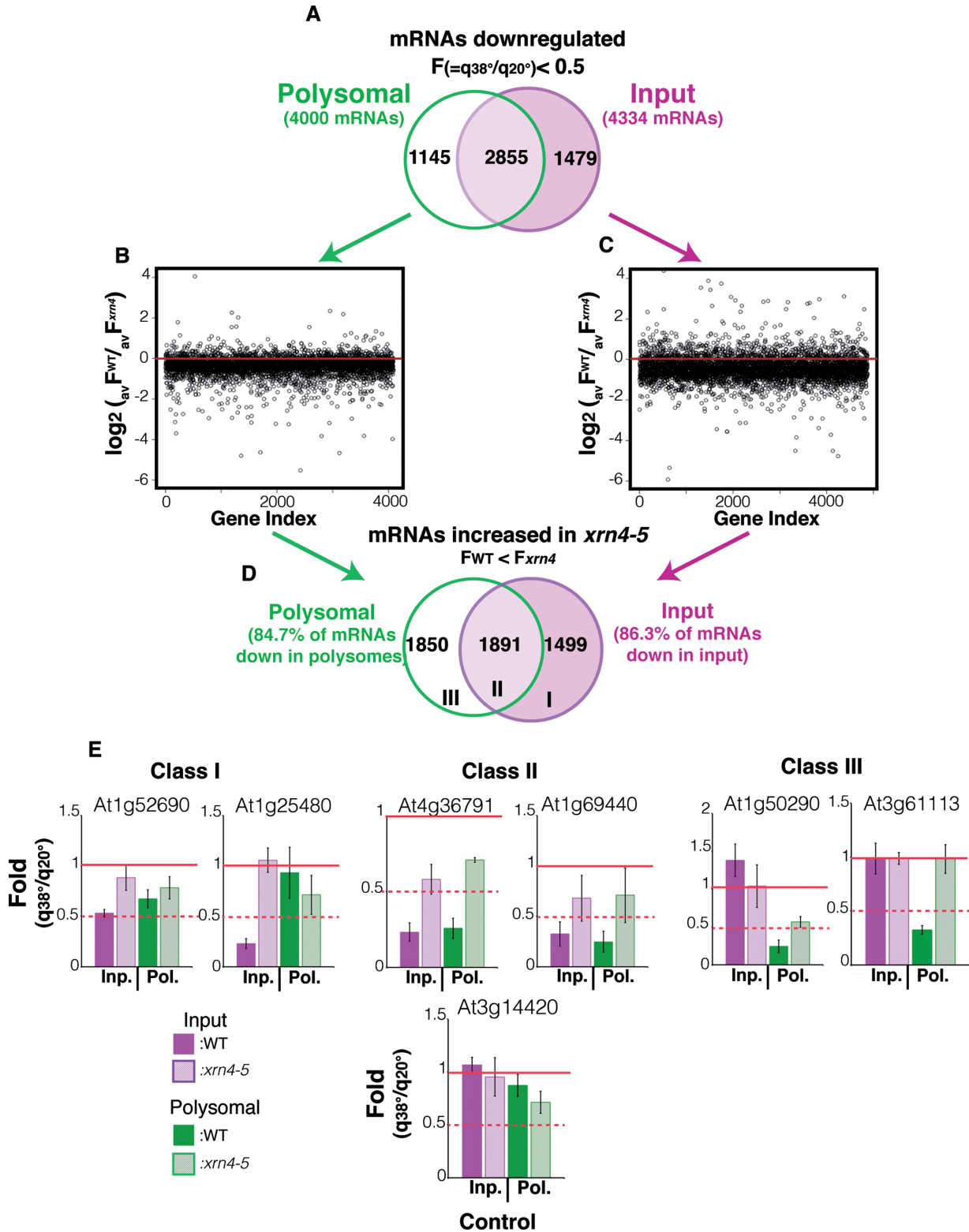


Figure 1. Heat stress triggers an XRN4-dependent mRNA downregulation in polysomes. (A) Venn diagram representation of the number of genes downregulated more than 2-fold in Polysomal (green) and/or Input (pink) fractions. Comparison of the fold ($q^{38^\circ} / q^{20^\circ}$) in wild-type and in *xrn4-5* for genes downregulated by heat in Polysomal (B) or Input fractions (C). The x axis is the gene index and the y axis is the value for the $\log_2(\frac{F_{WT}}{F_{xrn4-5}})$. (D) Venn diagram representation of the number of genes downregulated in polysomes and sensitive to *xrn4* knockout (with $\log_2(\frac{F_{WT}}{F_{xrn4-5}}) > 0$) (in green) and/or gene downregulated in input and sensitive to *xrn4* knockout (in pink). (E) qRT-PCR analyses of fold ($q^{38^\circ} / q^{20^\circ}$) variations for randomly chosen mRNAs from class I, II or III plus a control transcript (At3g14420) in wild-type (solid bars) or *xrn4-5* (hatched bars) in input (pink bars) or polysomes (green bars). qRT-PCR values were normalized to ACTIN 7 (At5g09810) and calculated as $q = 2^{(C_{Ref} - C_{Gene})}$. Values reported are the mean values of the folds, respectively, calculated from three biologically independent experiments. Standard deviations are shown.

samples, prepared in triplicate. We assessed level variations for 12 mRNAs randomly chosen from all three classes (four from each class) plus for a control transcript not targeted by XRN4 during heat stress (Figure 1E, Supplementary Figure S3F). Observation of the solid bars (corresponding to the wild-type background) on the histograms shows that mRNA levels decrease at least 2-fold, as predicted by RNA-seq analyses. The loss of XRN4 (hatched bars) has a significant impact only in the input fraction for class I, in the polysomal fraction for class III and in both for class II. Transcript levels are not systematically reestablished to that of unstressed levels in *xrn4-5* seedlings, supporting the existence of an XRN4-independent downregulation process. We also confirm that, as predicted by the RNA-seq data, At3g14420 is not a target of XRN4 in input nor in polysomal fractions.

In summary these data show that the heat-induced decrease of mRNA levels in input and polysomes is directly or indirectly dependent upon XRN4 function. The impact of XRN4 is major although not exclusive, as more than 85% of the genes see their levels increase at 38°C in *xrn4-5* seedlings. Given our previous demonstration of the existence of an H-SMD (23), we postulate that XRN4 mediates the rapid degradation of these transcripts following a short exposure at 38°C.

Heat stress triggers the formation of polysome-associated decapped mRNA intermediates

In heat stress, the polysomal concentration of participants in cytoplasmic 5'-mRNA turnover such as XRN4, its heat-specific cofactor LARP1 but also the decapping holoenzyme (DCP1/DCP2), is increased while translation is globally repressed (23). This observation prompts us to postulate that the XRN4-mediated underaccumulation of mRNAs in polysomes might be the direct result of a co-translational degradative process. If this is indeed the case, we reasoned that decay intermediates (i.e. decapped mRNAs) should overaccumulate at 38°C in the polysomes of *xrn4-5* seedlings. To test this hypothesis we used an SL-RT-PCR assay (36). Briefly, an RNA anchor is ligated to the 5'-monophosphate extremity of decapped mRNAs. The ligation is guided by a complementary splint DNA oligonucleotide, which bridges the 5'-end of the transcript of interest to the 3'-extremity of the anchor and allows the use of DNA rather than RNA ligase. After ligation, the splint is digested, the RNA reverse transcribed with a gene-specific primer (GSP, see Figure 2C) located at the 3'-end of the transcript, and cDNAs detected by PCR. Since only 5'-monophosphate molecules that fully hybridized with the mRNA-specific portion of the splint will be ligated to the anchor, a PCR signal with Pa (anchor primer) will be amplified only for decapped molecules. This technique hence allows the accurate and quantitative detection of the decapped (i.e. full length 5'-monophosphate forms) molecules in the total pool of a transcript of interest. We tested the accumulation of decapped decay intermediates for three input (class I) and three polysomal (class III) specific mRNAs (Figure 2 and Supplementary Figure S4A). We ran our assays on input and polysomal extracts prepared from control or heat stressed seedlings from either wild-type or

xrn4-5 backgrounds. No specific PCR signal is detected in any wild-type condition (Figure 2 and Supplementary Figure S4A, lanes 1, 2, 5, 6) whereas the TAP controls and internal PCRs are positive. This is expected since decapped forms if any are likely to be degraded by 5'-3' exoribonuclease activity of XRN4 (16). Except for At3g48410 which shows a faint PCR signal, inactivation of XRN4 at 20°C does not allow detection of decapped mRNAs in the input nor in polysomal fractions (Figure 2 and Supplementary Figure S4A, lanes 3 and 7), suggesting that the tested mRNAs are not decapped and/or below detection using a PCR-based approach at this temperature. By contrast, XRN4 depletion induces the accumulation (or overaccumulation in the case of At3g48410) of class I mRNAs PCR signals for 'splint assays' in the input, but not in the polysomal fraction (Figure 2A and Supplementary Figure S4A, lanes 4 and 8) and vice versa for class III transcripts (Figure 2B and Supplementary Figure S4A, lanes 4 and 8). Since the negative 'no ligase' controls do not allow any specific PCR signal to be detected, these amplifications actually reflect the presence of decapped mRNAs. These results show that decay intermediates overaccumulate in an XRN4-dependent manner at 38°C either in the input or polysomal fraction in agreement with the sub-cytoplasmic location where the transcripts were found to be sensitive to XRN4 depletion (Figure 1E and Supplementary Figure S3F). We previously demonstrated through direct measurement of mRNA half-lives that transcripts in the total fraction are downregulated by heat through an accelerated degradation mediated by XRN4 (23). The results of the SL-RT-PCR assays are consistent with these data and strongly support that, at least for the tested transcripts, the XRN4-mediated downregulation of mRNAs in polysomes upon heat stress is through direct 5'-3' degradation.

Heat exposure induces ribosome pausing and concomitant co-translational decay

Perturbations of the translational activity can be visualized on polysome profiles obtained following sucrose gradient separation. Observation of 'polysome traces' (Figure 3A) shows that heat induces a global decrease in polyribosomes and a concurrent increase in 80S monosomes and free ribosomal subunits consistently with impediment of translation initiation. This phenotype is proportional to the stress duration: the longer the exposure to heat, the stronger the polysome profile is altered (Figure 3B). An increased magnification of the region of the polysome profile encompassing peaks 1-4 shows that the light polysomes (which correspond to mRNAs loaded with two to five ribosomes) do not drop and are even more abundant at 38°C than at 20°C (Figure 3A). We can observe similar polysome profiles in the *xrn4-5* genetic background (compare left to right panel of Figure 3A), suggesting that the loss of XRN4 has no measurable impact on global polysomal profile, at least at this level of resolution. We next run a time course by exposing *xrn4-5* seedlings for 10, 20 and 30 min at 38°C and quantified the amounts of light and total polyribosomes relative to amounts at 20°C (Figure 3B-D). Since absorbance at 254 nm directly correlates with amount of nucleic and amino acids present in the sample, the rela-

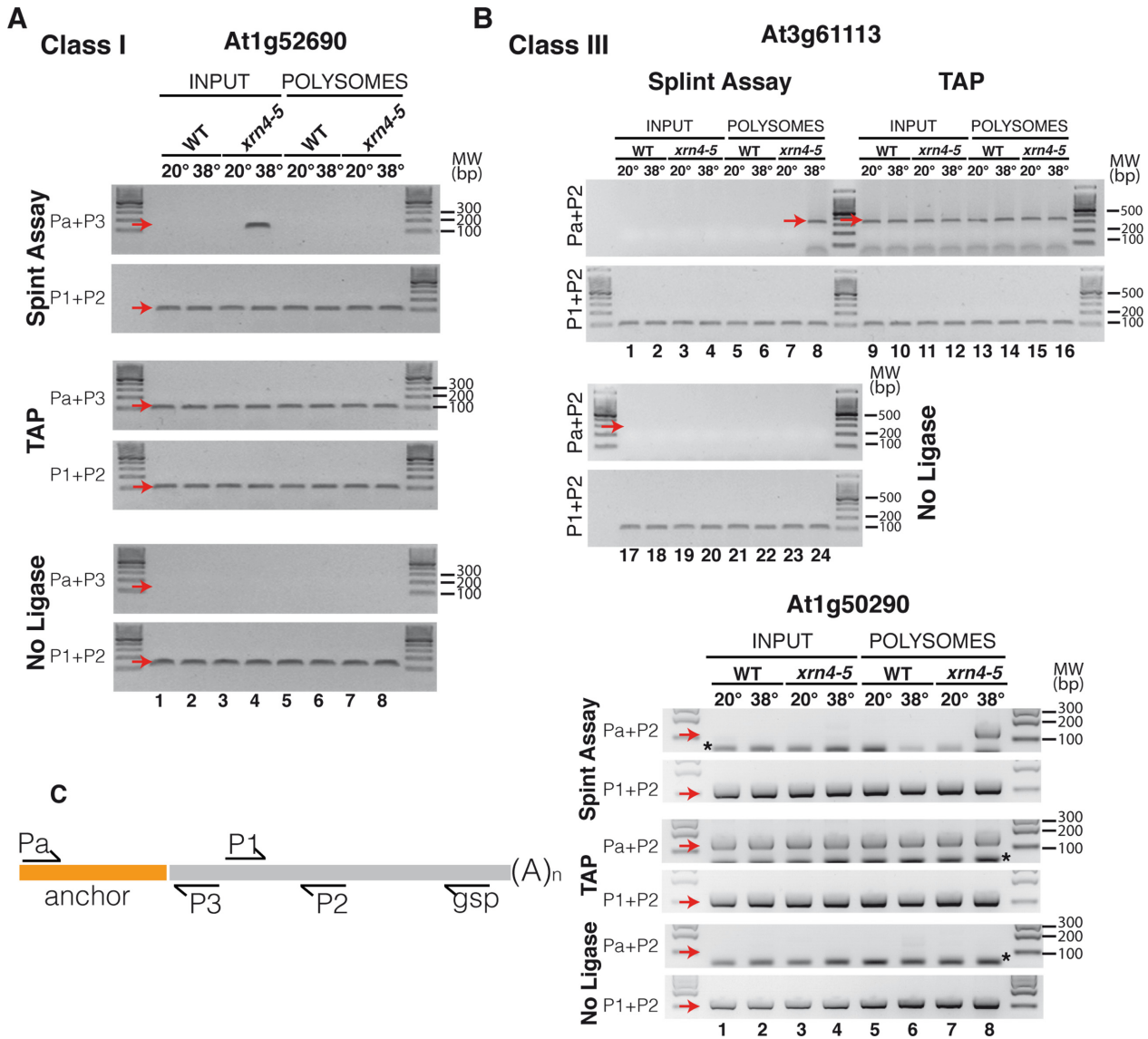


Figure 2. Heat triggers the overaccumulation of decapped mRNAs in *xrn4-5* seedlings. Spint Ligation(SL)-RT-PCR assays for a class I At1g52690 (A) and two class III (At3g61113, At1g50290) (B) mRNAs. Assays were conducted on input (lanes 1–4) and polysomal (lanes 5–8) RNAs prepared from the same crude extract from seedlings (wild-type or *xrn4-5*) either control (20°C, odd lanes) or heat treated for 30 min at 38°C (even lanes). From a same preparation, RNAs were either mock treated (spint assay) or TAP treated (TAP) before SL-RT-PCR, or ligase was omitted during the SL step (no ligase). After SL, RTs were primed with GSP. Subsequently, PCRs were conducted with primers Pa and P2 or P1 and P2. Red arrows mark the positions of the specific PCR products and asterisks mark the position of nonspecific primer dimers signal. (C) Diagram representing the positions of the primers used to detect cDNAs produced from decapped mRNAs or from the total pool of mRNA. The GSP was used for reverse transcription after ligation of the spint DNA. PCR with (Pa+P2) or (Pa+P3) allows to detect cDNA with an anchor sequence: corresponding to decapped mRNA. PCR with (P1+P2) is used to monitor the presence of cDNA with or without anchor representing the whole pool (capped plus decapped) of a given transcript.

tive amount of polysomes can be estimated through measurement of the area covered between the polysome profile curve and the basal line (Figure 3C). For each time point, we calculated independently the area covered by peaks 1–4 (the light polysomes) and by the total polyribosomes. To clearly evaluate the impact of temperature increase, we normalized each stress value to its corresponding unstressed value (Figure 3C). As expected, the total amount of polyribosomes shows a constant decrease over the time of exposure at 38°C. By contrast the amount of two, three and four ribosomes containing polysomes (peaks 1, 2 and 3) overaccumulate as soon as 10 min after heat stress induction.

Between 20 and 30 min, the amount of light polysomes progressively decrease but the amount of mRNAs engaged with two polysomes (peak 1) still remains more important after 30 min at 38°C compared to the 20°C reference. Also, the decrease rate of light polysomes, including peak number 4, is slower than that of the total polysomes. To confirm this result another way, we normalized the area covered by each peak to that covered by total polyribosomes (to directly quantify the relative contribution of each light polysomal species to the whole polyribosomes amount at 38°C) and again draw a comparison to the unstressed values by setting those values to 1 (Figure 3D). We observe

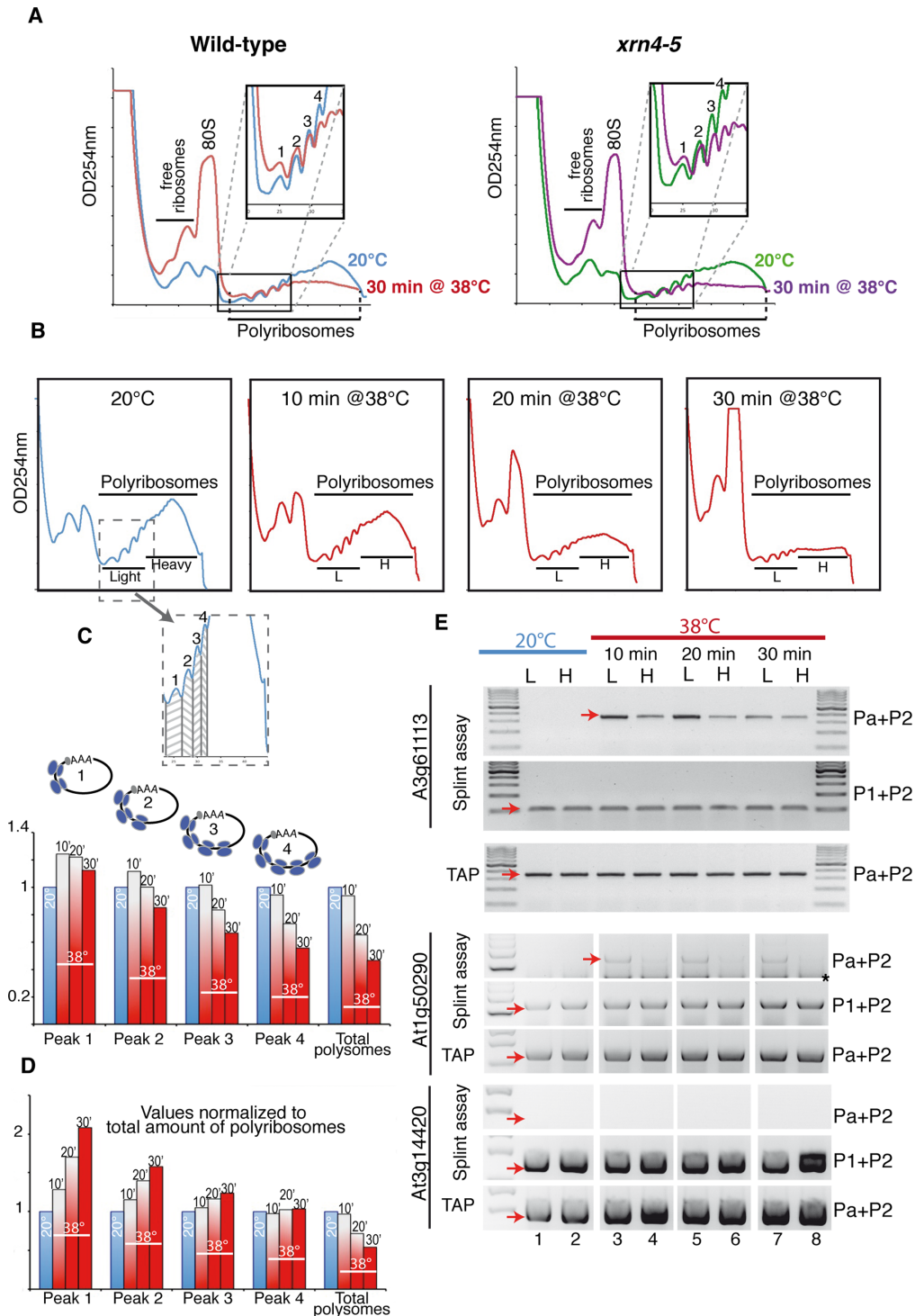


Figure 3. Heat triggers ribosome pausing and co-translational decay. (A) Polysome profiles were determined using sucrose gradient sedimentation and OD_{254nm} measurement for wild-type (left panel) or *xrn4-5* (right panel) seedlings incubated 30 min at 20°C (blue and green profiles) or 38°C (red and purple profiles). A magnification of the profiles around light polysomes is shown above each graph. (B) Polysome profiles from *xrn4-5* seedlings either control (20°) or treated 10, 20 or 30 min at 38°C. The positions of the light (L) and heavy (H) polysomes are shown on the graph. (C, D) Amounts of light polysomes (peaks 1, 2, 3 and 4 representing mRNAs loaded with 2, 3, 4 and 5 ribosomes) and total polyribosomes normalized to the corresponding values at 20°C. Amount of polysomes were estimated by measurement of the area comprised between the polysome profile and the basal line (hatched areas shown in the magnified window). (C) Area values were either normalized to 20°C values or (D) calculated as a percentage of the total polyribosomes and normalized to the corresponding percentage at 20°C. (E) SL-RT-PCR assays conducted on RNAs extracted from light (L: odd lanes) and heavy (H: even lanes) *xrn4-5* polysome fractions collected after sucrose gradients which profiles are shown in B. From a same preparation, RNAs were either mock treated (Splint assay) or TAP treated (TAP) before SL-RT-PCR, or ligase was omitted before the SL step (data not shown). Assays were performed for two class III (At3g61113 and At1g50290) and a control (At3g14420) mRNA. Names of the primers are as in Figure 2. Red arrows mark the positions of the specific PCR products and asterisks mark the position of nonspecific primer dimers signal.

that, under conditions where the total amount of polysomes is dropping rapidly, the relative areas covered by peaks 1–3 are increasing over time, while that covered by peak 4 remains constant. This proves that light polysomes are clearly overrepresented at 38°C (this is particularly obvious after 20 and 30 min of treatment) and that consequently the proportion of heavy polysomes is dropping faster than that of light polysomes during heat stress. This suggests that in plants like in animals, heat alters elongation rates differentially along the transcript. Amongst various possible scenarios we postulate that we are observing a 5'-ribosome pausing phenomenon (see the Discussion), which results in an accumulation of ribosomes upstream and depletion of ribosomes downstream of the trapping point (6,7).

It is not yet clear at present how mRNAs still actively translated can be at the same time target for degradation (25). We postulate that alterations of elongation rates might favor polysomal decay by inducing decapping and degradation. If this is the case, then full length decapped decay intermediates should preferentially appear in light polysome fractions in *xrn4-5*. To test this hypothesis, we separately purified RNAs from light and heavy fractions prepared from control (20°C) and 38°C exposed *xrn4-5* seedlings and checked 5'-decay intermediates accumulation by SL-RT-PCR assay (Figure 3E, Supplementary Figure S4B). While no decapped transcript can be detected in any polysomal fraction at 20°C (lanes 1 and 2, Figure 3E, Supplementary Figure S4B), 5'-unprotected mRNAs are detected at 38°C as soon as 10 min after beginning of the stress treatment (lanes 3 and 4, Figure 3E, Supplementary Figure S4B). Both polysome specific XRN4-targets (At3g61113, At1g50290 and At5g49480) accumulate more decapped molecules in the light than heavy fractions after 10 and 20 min at 38°C (Figure 3E and Supplementary Figure S4B). The control At3g14420 mRNA, that is not a target of XRN4 (Figure 1E), does not show any 5'-unprotected transcript accumulation in any polysomal fraction (Figure 3E).

All in all, these data suggest that transcripts that are degraded in polysomes accumulate preferentially in light than in heavy fractions. Also, the kinetic analysis shows that decay intermediates can be detected very early in the course of stress exposure, concomitantly with ribosome pausing. These observations support the hypothesis of a direct link between the heat induced 5'-ribosome slowing phenomenon and the co-translational decay process.

HSP70 inactivation results in ribosome pausing and co-translational decay

We next sought to get a better understanding of why an mRNA would be preferentially degraded in polysomes. A Gene Ontology search revealed that class III is enriched for mRNA coding for proteins predicted to be part of the endomembrane system (P -value $4.7 \cdot 10^{-8}$) (Supplementary Figure S5A). This is not the case for class I mRNAs that do not show any highly significant term enrichment for this 'Cellular Component' category (Supplementary Figure S5B). Work from Shalgi *et al.* (7) and Liu *et al.* (6) demonstrated that stress triggered 5'-ribosome pausing is preferentially set up on mRNAs that code for products with hydrophobic N-termini and tend to be more dependent upon

HSC70/HSP70 chaperone activities. We hence determined the hydrophobicity and HSC70/HSP70 affinity scores of N-terminal peptides of class III and class I gene products (Figure 4A and B). We found that mRNAs targeted by XRN4 in polysomes are associated with higher hydrophobicity (t-test P -value of $3.9 \cdot 10^{-3}$) and better HSC70/HSP70 binding scores (t-test P -value of $1.2 \cdot 10^{-10}$) than those only targeted in the cytoplasm (Figure 4A and B). These results are consistent with the enrichment we found for mRNAs coding for endomembrane proteins in class III, and suggest that, in Arabidopsis also, pausing might be related to the hydrophobic status of N-terminal peptides and to HSC/HSP70 dependency. VER-155008 is an adenosine-derived specific inhibitor of the HSC70 and HSP70 proteins. It does not affect their interaction with cochaperones but acts through direct inhibition of their ATPase activity by inserting into their nucleotide-binding site and competing with ATP (37,38). Co-crystal structure analyses demonstrated that VER-155008 fits between two residues and forms hydrogen bonding with three residues, all highly conserved, of the ATP binding pocket of HSP70 ((37,38), Supplementary Figure S5C and D). Its mode of action is hence highly specific and likely evolutionarily conserved. The Arabidopsis genome encodes three constitutive cytoplasmic HSC70 and two heat inducible HSP70 proteins, which have a very high level of sequence identity with their human orthologues (Supplementary Figure S5C). In particular, the residues found to be involved in VER-155008 binding are 100% conserved in plant proteins. We found that seedlings germinated in the dark remain etiolated when treated with VER-155008 and that heat-treated seedlings exposed to VER-155008 do not recover as well as mock-treated plants (data not shown). These and the specific sequence conservation of their ATPase domain (other chaperones such as HSP90 and HSP101 have a very different ATPase domain) support that VER-155008 also acts as a specific inhibitor of HSC/HSP70 in Arabidopsis. To analyze the impact of inhibiting HSC/HSP70 chaperone activity on 5'-ribosome pausing, we incubated *xrn4-5* seedlings for 60 min at 20°C in liquid medium containing either 100 μM VER-155008 (VER) or 0.1% DMSO as control treatment, prepared polysomal extracts and ran analytical sucrose gradients. Polysome profile analyses conducted in three independent replicates (Figure 4C) and data not shown) show that VER treatment induces a reproducible decrease in heavy polysome fractions and an increase in light polysomes (peaks 1–4). This can be also visualized by subtracting the VER sample Optical Density (OD) values from control sample (orange curve on polysome profile of Figure 4C). In contrast to the heat stress treatment (Figure 3A), the drug treatment does not appear to influence the translation initiation step since the drop in polyribosome levels is not accompanied by an increase in monosomes nor free ribosomes. Accordingly, treatment for 60 min with 100 μM VER does not induce the formation of SG in contrast to the heat treatment (Supplementary Figure S5E). All this suggests that HSC/HSP70 chaperone activity inhibition affects translation but most likely at a post-initiation step. In addition, as it is the case in mammals (6,7), this also seems to induce differential alterations of the elongation rates along the open reading frame.

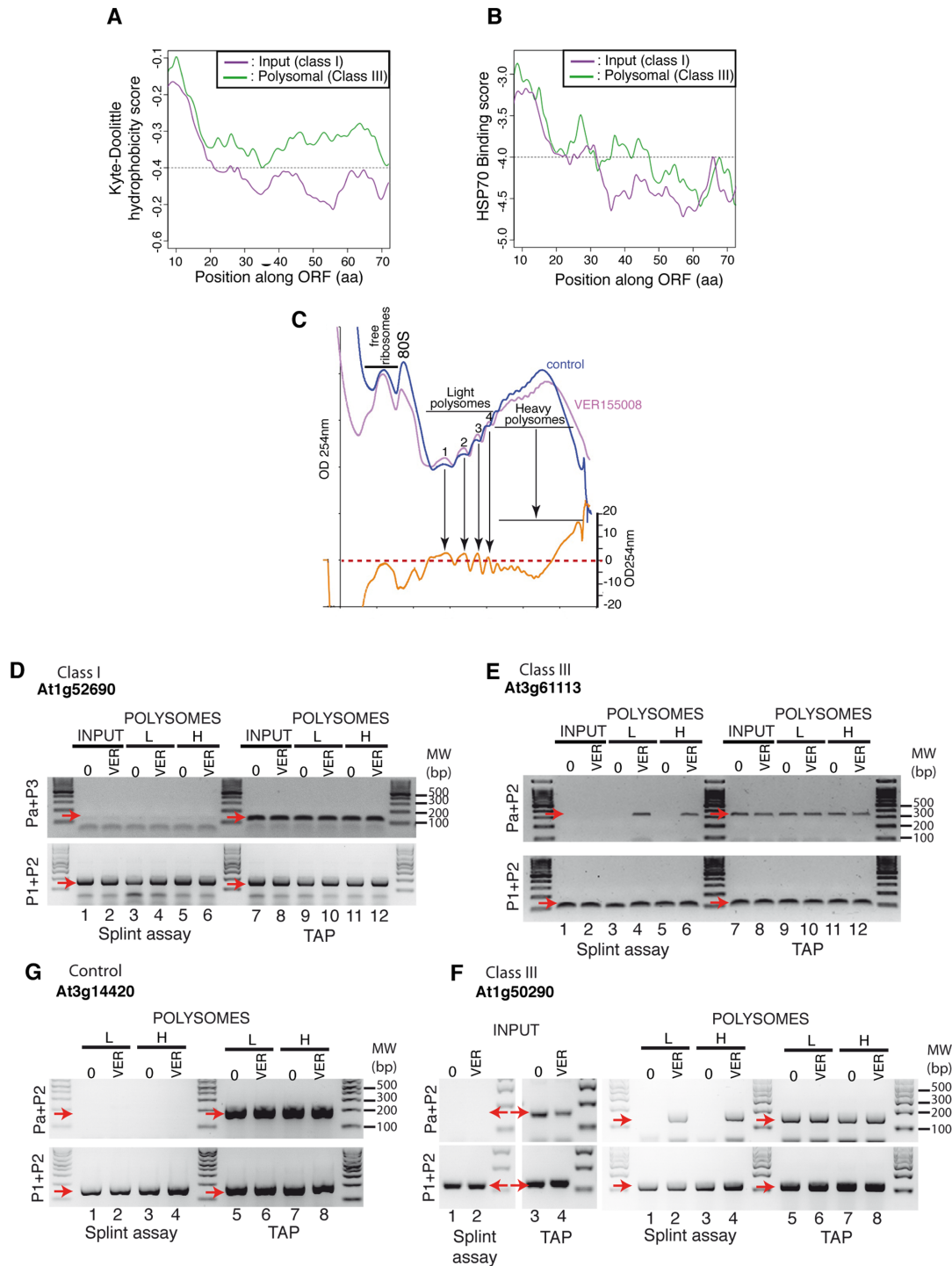


Figure 4. HSC/HSP70 inactivation triggers ribosome pausing and XRN4-mediated co-translational decay. (A) Hydrophobicity and (B) HSC/HSP70 binding scores for the first 80 amino acids encoded by genes specifically targeted by XRN4 in input (class I) (pink) or in polysomes (class III) (green). Scores were calculated for 13 amino acids long windows sliding by one amino acid along the first 80 amino acids of the proteins coded by class I and class III genes. The mean values calculated between members of each subgroup are reported. T-test *P*-values for the differences between the mean scores of XRN4 input and polysome targets were $3.9 \cdot 10^{E3}$ for hydrophobicity and $1.2 \cdot 10^{E10}$ for HSC/HSP70 binding. (C) Polysome profiles determined by sucrose gradient sedimentation and OD_{254nm} measurement for wild-type seedlings treated at 20°C for 60 min with 100 μM VER155008 (pink line) or with DMSO (control; blue line). Orange profile shown at the bottom of the graph corresponds to the subtraction of the VER-155008 profile from the control profile. The y axis for this subtraction profile is shown on the right-hand side. (D–G) Monitoring of decapped species accumulation. Crude polysomal extracts were prepared from *xrn4-5* seedlings either DMSO (control: (0)) or 100 μM VER155008 (VER) treated for 60 min at 20°C. SL-RT-PCR assays were performed on RNAs recovered from crude extracts (Input) or from Light and Heavy polysomes following sucrose gradients separation. For each RNA sample, a positive TAP treated reaction (TAP) and a negative ‘no ligase’ (Supplementary Figure S6) reaction have been conducted. (D) Results for a class I mRNA (At1g52690) in input and polysomes, (E, F) results for class III (At3g61113 and At1g50290) mRNAs in input and polysomes, (G) results for the control At3g14420 mRNA in polysomes. Names of the primers are as in Figure 2. Red arrows mark the positions of the specific PCR products.

If our working model is correct, VER-155008 treatment should not only induce ribosome pausing but also polysomal degradation of transcripts in which translation elongation is altered. We explored this hypothesis by conducting SL-RT-PCR experiments to detect decay intermediates in the input, light and heavy polysome fractions prepared from *xrn4-5* seedlings either mock or VER treated at 20°C for 60 min (Figure 4D–F and Supplementary Figure S6A). The class III At3g61113 (Figure 4E, lanes 4 and 6), At1g50290 (Figure 4F, lanes 6, 8) and At5g49480 (Supplementary Figure S6A, lanes 4 and 6) transcripts show a clear overaccumulation of decapped molecules in the light and heavy polysome samples following VER-mediated hindering of HSC/HSP70 activity. The appearance of 5'-decay intermediates is specific to polysomal fractions, as no PCR signal is detected when probing the input samples either mock- or VER-treated (Figure 4E, F and Supplementary Figure S6A, lanes 1 and 2). Moreover, neither the input specific target of XRN4 (At1g52690) nor the nonsensitive control mRNA (At3g14420) shows accumulation of decapped molecules following drug treatment whatever the sample analyzed (Figure 4D and G). Samples where ligase was omitted (i.e. without an anchor ligated) show no PCR signal, except when the internal control primers (P1–P2) were used (Supplementary Figure S6), demonstrating that the PCR signal observed are specific to accumulating decapped forms. In conclusion these SL-RT-PCR experiments show that VER treatment triggers at 20°C the accumulation of 5'-decay intermediates in polysomes for transcripts we found to be co-translationally degraded during heat stress.

Overall, our results suggest that 5'-ribosome pausing, whether induced by heat or by inhibiting HSC/HSP70 activity, favors degradation of specific mRNAs in polysomes.

DISCUSSION

The data we present here support that XRN4 is a stress responsive protein which function is reprogrammed by heat sensing. While its loss of function appears to affect only a limited number of poly(A)-affinity purified mRNAs at 20°C, several thousand transcripts see their levels increase at 38°C, supporting the global involvement of XRN4 in the H-SMD (23). We also provide evidence that the H-SMD mechanism requires an initial decapping step prior to the 5'-directed digestion of the heat targeted transcripts. Our results also strongly suggest that H-SMD not only takes place in the cytoplasm but also on mRNAs still engaged in polysomes.

Heat stress induces a reduction in cellular translational activity that expectedly results in a diminution of the amount of mRNAs associated with polyribosomes (5,39,40). What is more unexpected is our observation that this downregulation is globally (although not exclusively) dependent upon the presence of the XRN4 exoribonuclease. Based on this result, we propose that heat not only directly affects mRNA engagement in polysomes through translation initiation inhibition but also triggers their co-translational decay. We provide a direct proof of this by detecting 5'-decay intermediates of randomly chosen transcripts in polysomes of XRN4-depleted seedlings. It is unlikely that the observed XRN4-mediated increase of tran-

scripts in polysomes is non-specifically linked to sedimentation of p-bodies RNP aggregates in the high-density layers of the sucrose gradient. Indeed if this were the case, we would not be able to observe an overaccumulation of polysomal decapped mRNAs following VER155008 treatment as this drug does not inhibit translation initiation a condition required to stimulate the formation of RNP granules of p-bodies and SG type (data not shown and Supplementary Figure S5E). Moreover, we have demonstrated previously that, despite a general diminution of polyribosome levels, there is a higher fraction of XRN4 and DCP1/DCP2 specifically associated with translating mRNAs in heat stress, supporting a direct role for these factors in polysomes (23). All in all, our data support the hypothesis that heat provokes a co-translational decay process through which mRNAs are digested by XRN4, most likely following a decapping step. The existence of a co-translational decay process was previously established in yeast (32) but we provide here the first demonstration that it can affect a large number of endogenous mRNAs and that it likely plays a role in the cellular adaptation to stress. Previous reports not only detected a polysomal association for several mRNA decay factors or cofactors either in human (33) or yeast (41,42) but also showed that their polysomal concentration increases when translation decreases in salt stress (42) or at diauxic shift (41). This suggests that the stress-induced co-translational decay might be an evolutionarily conserved phenomenon with significant physiological consequences.

Like in animals, heat seems to have an elaborate impact on translation in *A. thaliana*, not only by blocking initiation but also by differentially affecting elongation along the coding region of the messenger. One could imagine that the increase in light ribosomes we observed after 30 min of heat stress is simply due to mRNAs shifting to lighter fractions of the sucrose gradient because ribosomes are running off and are not reloaded as translation initiation is blocked. However, based on Arabidopsis CDS sizes (75% being shorter than 2000 bp (TAIR10: <ftp://ftp.arabidopsis.org/home/tair/Sequences/>)) and on the normal rate of translation (5–6 amino acids per second (8)), no ribosome should remain on most mRNAs, 2 min following translation inhibition. Therefore, the presence of numerous transcripts still engaged with ribosomes 30 min after heat stress is likely the result of a slowdown in translation elongation rate. Since these mRNAs are mainly engaged with two to five ribosomes as in (6,7) and since an eukaryotic ribosome protects some 30 nucleotides (43), we deem likely that this slowdown in translation elongation rate occurs, in plants as in animals, around codon 65. We cannot exclude that the elongation rate after this position is increased by stress, but for the very same mathematical calculation as before, translation velocity has to be severely reduced for the light polysome fractions to remain at such high levels after 30 min of stress exposure.

We also show that chemically hindering HSC/HSP70 chaperone activity has similar impact on elongation rates as heat, without affecting primarily translation initiation. Moreover, we found that plant cytosolic HSC/HSP70 proteins associate with polysomes (data not shown). This, together with the fact that the requirement for HSC/HSP70

for proper folding of the nascent polypeptide is conserved from yeast to human (8,44), suggests that plant HSC/HSP70 chaperoning also acts at the ribosome exit tunnel. All in all, our data support a model in which, in plants as in animal cells, heat triggers a 5'-ribosome pausing phenomenon leading to the modulation of translation elongation due, at least in part, to an HSC/HSP70-dependent sensing activity.

Hindering HSC/HSP70 activity causes 5'-ribosome pausing and allows the polysomal accumulation of decay intermediates only for class III mRNAs. In heat situation, there is a concomitant appearance of paused ribosomes and 5'-decay intermediates in polysomes. Class III mRNAs code for proteins with biochemical properties (hydrophobicity, HSC/HSP70 binding score) similar to those found to be most sensitive to heat induced pausing in animals (7). Put together these data strongly support that, in response to stress inducing 5'-ribosome pausing, mRNAs are recognized for decapping and XRN4 digested. Under our heat stress condition, XRN4-mediated decay is unlikely to take place after paused ribosomes are dissociated, as it is the case for aberrant mRNA degradation (of No-Go and Non-Stop decays) (45,46), otherwise XRN4 sensitive transcripts would not increase in polysomal fractions. Since heat and proteotoxic stresses likely slow rather than stall elongation (6,7), XRN4, once recruited at the 5'-end of decapped molecules, could simply degrade these mRNAs simultaneously as ribosomes slowly move along the transcript.

In summary, our work provides evidence that the co-translational mRNA degradation process first found to exist in *S. cerevisiae* on a limited number of transcripts (32) is physiologically relevant in response to heat stress and affects several thousand mRNAs. We show that it is intertwined with the HSP70-dependent ribosome pausing phenomenon which we propose to constitute the signal that targets mRNAs for polysomal degradation. Translation activity and mRNA fate are interrelated. Translation stalling is now clearly defined as the signal that marks an aberrant transcript for degradation (46). Our data support that translation efficiency also governs the fate of a large number of otherwise non-aberrant mRNAs marking them for rapid decay as part of the cellular response to stress. Finally, our work also rises the exciting possibility that inappropriate folding of emerging polypeptides could directly feedback on the stability of their coding transcripts and posits the HSC/HSP70 chaperone as a stress sensing hub dispatching signal to reprogram mRNA stability.

SUPPLEMENTARY DATA

Supplementary Data are available at NAR Online.

ACKNOWLEDGEMENT

We would like to thank Marie Mirouze from critical reading of the manuscript. We also thank Dr Shu-Hsing Wu (IPMB, Academia Sinica, Taiwan) for granting the first author access to her gradient fractionator.

FUNDING

l'Agence Nationale pour la Recherche (ANR-2010 BLANC 1707 01, ANR Heat-Adapt ANR -14-CE10-0015); Centre National pour la Recherche Scientifique (CNRS); Université de Perpignan Via Domitia (UPVD) through utilization of the confocal microscope and qPCR devices at the Techno-viv platform; National Science Foundation [MCB-1021636 to P.J.G.]. Funding for open access charge: French Agence Nationale pour la Recherche (ANR) and National Scientific Research Centre (CNRS).

Conflict of interest statement. None declared.

REFERENCES

- Larkindale, J. and Vierling, E. (2008) Core genome responses involved in acclimation to high temperature. *Plant Physiol.*, **146**, 748–761.
- Kotak, S., Larkindale, J., Lee, U., von Koskull-Doring, P., Vierling, E. and Scharf, K.D. (2007) Complexity of the heat stress response in plants. *Curr. Opin. Plant Biol.*, **10**, 310–316.
- Mittler, R., Finka, A. and Goloubinoff, P. (2011) How do plants feel the heat? *Trends Biochem. Sci.*, **37**, 118–125.
- Liu, B. and Qian, S.B. (2014) Translational reprogramming in cellular stress response. *Wiley Interdiscip. Rev. RNA*, **5**, 301–315.
- Munoz, A. and Castellano, M.M. (2012) Regulation of translation initiation under abiotic stress conditions in plants: is it a conserved or not so conserved process among eukaryotes? *Comp. Funct. Genomic*, **2012**, 406357.
- Liu, B., Han, Y. and Qian, S.B. (2013) Cotranslational response to proteotoxic stress by elongation pausing of ribosomes. *Mol. Cell*, **49**, 453–463.
- Shalgi, R., Hurt, J.A., Krykbaeva, I., Taipale, M., Lindquist, S. and Burge, C.B. (2013) Widespread regulation of translation by elongation pausing in heat shock. *Mol. Cell*, **49**, 439–452.
- Kramer, G., Boehringer, D., Ban, N. and Bukau, B. (2009) The ribosome as a platform for co-translational processing, folding and targeting of newly synthesized proteins. *Nat. Struct. Mol. Biol.*, **16**, 589–597.
- Jaiswal, H., Conz, C., Otto, H., Wolffe, T., Fitzke, E., Mayer, M.P. and Rospert, S. (2011) The chaperone network connected to human ribosome-associated complex. *Mol. Cell Biol.*, **31**, 1160–1173.
- Otto, H., Conz, C., Maier, P., Wolffe, T., Suzuki, C.K., Jenö, P., Rucknagel, P., Stahl, J. and Rospert, S. (2005) The chaperones MPP11 and Hsp70L1 form the mammalian ribosome-associated complex. *Proc. Natl Acad. Sci. U.S.A.*, **102**, 10064–10069.
- Belostotsky, D.A. and Sieburth, L.E. (2009) Kill the messenger: mRNA decay and plant development. *Curr. Opin. Plant Biol.*, **12**, 96–102.
- Chiba, Y. and Green, P.J. (2009) mRNA degradation machinery in plants. *J. Plant Biol.*, **52**, 114–124.
- Garneau, N.L., Wilusz, J. and Wilusz, C.J. (2007) The highways and byways of mRNA decay. *Nat. Rev. Mol. Cell Biol.*, **8**, 113–126.
- Parker, R. (2012) RNA degradation in *Saccharomyces cerevisiae*. *Genetics*, **191**, 671–702.
- Nagarajan, V.K., Jones, C.I., Newbury, S.F. and Green, P.J. (2013) XRN 5'→3' exoribonucleases: structure, mechanisms and functions. *Biochim. Biophys. Acta*, **1829**, 590–603.
- Kastenmayer, J.P. and Green, P.J. (2000) Novel features of the XRN-family in Arabidopsis: evidence that AtXRN4, one of several orthologs of nuclear Xrn2p/Rat1p, functions in the cytoplasm. *Proc. Natl Acad. Sci. U.S.A.*, **97**, 13985–13990.
- Kastenmayer, J.P., Johnson, M.A. and Green, P.J. (2001) Analysis of XRN orthologs by complementation of yeast mutants and localization of XRN-GFP fusion proteins. *Methods in enzymology*, **342**, 269–282.
- Souret, F.F., Kastenmayer, J.P. and Green, P.J. (2004) AtXRN4 degrades mRNA in Arabidopsis and its substrates include selected miRNA targets. *Mol. Cell*, **15**, 173–183.
- Arribas-Layton, M., Wu, D., Lykke-Andersen, J. and Song, H. (2013) Structural and functional control of the eukaryotic mRNA decapping machinery. *Biochim. Biophys. Acta*, **1829**, 580–589.

20. Goeres, D.C., Van Norman, J.M., Zhang, W., Fauver, N.A., Spencer, M.L. and Sieburth, L.E. (2007) Components of the Arabidopsis mRNA decapping complex are required for early seedling development. *Plant Cell*, **19**, 1549–1564.
21. Xu, J., Yang, J.Y., Niu, Q.W. and Chua, N.H. (2006) Arabidopsis DCP2, DCP1, and VARICOSE form a decapping complex required for postembryonic development. *Plant Cell*, **18**, 3386–3398.
22. Balagopal, V., Fluch, L. and Nissan, T. (2012) Ways and means of eukaryotic mRNA decay. *Biochim. Biophys. Acta*, **1819**, 593–603.
23. Merret, R., Descombin, J., Juan, Y., Favory, J.-J., Carpentier, M.-C., Chaparro, C., Charng, Y., Deragon, J.-M. and Bousquet-Antonelli, C. (2013) XRN4 and LARP1 are required for a heat-triggered mRNA decay pathway involved in plant acclimation and survival during thermal stress. *Cell Rep.*, **5**, 1279–1293.
24. Huch, S. and Nissan, T. (2014) Interrelations between translation and general mRNA degradation in yeast. *Wiley Interdiscip. Rev. RNA*, **5**, 747–763.
25. Roy, B. and Jacobson, A. (2013) The intimate relationships of mRNA decay and translation. *Trends Genetics*, **29**, 691–699.
26. Bruno, I. and Wilkinson, M.F. (2006) P-bodies react to stress and nonsense. *Cell*, **125**, 1036–1038.
27. Weber, C., Nover, L. and Fauth, M. (2008) Plant stress granules and mRNA processing bodies are distinct from heat stress granules. *Plant J.*, **56**, 517–530.
28. Sheth, U. and Parker, R. (2003) Decapping and decay of messenger RNA occur in cytoplasmic processing bodies. *Science*, **300**, 805–808.
29. Brengues, M., Teixeira, D. and Parker, R. (2005) Movement of eukaryotic mRNAs between polysomes and cytoplasmic processing bodies. *Science*, **310**, 486–489.
30. Kulkarni, M., Ozgur, S. and Stoecklin, G. (2010) On track with P-bodies. *Biochem. Soc. Trans.*, **38**, 242–251.
31. Anderson, P. and Kedersha, N. (2008) Stress granules: the Tao of RNA triage. *Trends Biochem. Sci.*, **33**, 141–150.
32. Hu, W., Sweet, T.J., Chamnongpol, S., Baker, K.E. and Collier, J. (2009) Co-translational mRNA decay in *Saccharomyces cerevisiae*. *Nature*, **461**, 225–229.
33. Mangus, D.A. and Jacobson, A. (1999) Linking mRNA turnover and translation: assessing the polyribosomal association of mRNA decay factors and degradative intermediates. *Methods*, **17**, 28–37.
34. Mustroph, A., Juntawong, P. and Bailey-Serres, J. (2009) Isolation of plant polysomal mRNA by differential centrifugation and ribosome immunoprecipitation methods. *Methods Mol. Biol.*, **553**, 109–126.
35. Logemann, J., Schell, J. and Willmitzer, L. (1987) Improved method for the isolation of RNA from plant tissues. *Anal. Biochem.*, **163**, 16–20.
36. Blewett, N., Collier, J. and Goldstrohm, A. (2011) A quantitative assay for measuring mRNA decapping by splinted ligation reverse transcription polymerase chain reaction: qSL-RT-PCR. *RNA*, **17**, 535–543.
37. Schlecht, R., Scholz, S.R., Dahmen, H., Wegener, A., Sirrenberg, C., Musil, D., Bomke, J., Eggenweiler, H.M., Mayer, M.P. and Bukau, B. (2013) Functional analysis of Hsp70 inhibitors. *PLoS One*, **8**, e78443.
38. Williamson, D.S., Borgognoni, J., Clay, A., Daniels, Z., Dokurno, P., Drysdale, M.J., Foloppe, N., Francis, G.L., Graham, C.J., Howes, R. et al. (2009) Novel adenosine-derived inhibitors of 70 kDa heat shock protein, discovered through structure-based design. *J. Med. Chem.*, **52**, 1510–1513.
39. Matsuura, H., Ishibashi, Y., Shinmyo, A., Kanaya, S. and Kato, K. (2010) Genome-wide analyses of early translational responses to elevated temperature and high salinity in *Arabidopsis thaliana*. *Plant Cell Physiol.*, **51**, 448–462.
40. Yanguez, E., Castro-Sanz, A.B., Fernandez-Bautista, N., Oliveros, J.C. and Castellano, M.M. (2013) Analysis of genome-wide changes in the transcriptome of *Arabidopsis* seedlings subjected to heat stress. *PLoS One*, **8**, e71425.
41. Drummond, S.P., Hildyard, J., Firczuk, H., Reamtong, O., Li, N., Kannambath, S., Claydon, A.J., Beynon, R.J., Evers, C.E. and McCarthy, J.E. (2011) Diauxic shift-dependent relocalization of decapping activators Dhh1 and Pat1 to polysomal complexes. *Nucleic Acids Res.*, **39**, 7764–7774.
42. Sweet, T., Kovalak, C. and Collier, J. (2012) The DEAD-box protein Dhh1 promotes decapping by slowing ribosome movement. *PLoS Biol.*, **10**, e1001342.
43. Ingolia, N.T., Brar, G.A., Rouskin, S., McGeachy, A.M. and Weissman, J.S. (2012) The ribosome profiling strategy for monitoring translation in vivo by deep sequencing of ribosome-protected mRNA fragments. *Nat. Protoc.*, **7**, 1534–1550.
44. Hartl, F.U., Bracher, A. and Hayer-Hartl, M. (2011) Molecular chaperones in protein folding and proteostasis. *Nature*, **475**, 324–332.
45. Inada, T. (2013) Quality control systems for aberrant mRNAs induced by aberrant translation and termination. *Biochem. Biophys. Acta*, **1829**, 634–642.
46. Shoemaker, C.J. and Green, R. (2012) Translation drives mRNA quality control. *Nat. Struct. Mol. Biol.*, **19**, 594–601.